nature communications

Article

https://doi.org/10.1038/s41467-025-57206-w

Creation of a eukaryotic multiplexed site-specific inversion system and its application for metabolic engineering

Received: 23 May 2024

Accepted: 12 February 2025

Published online: 24 February 2025

Check for updates

Jieyi Li[1,2,3,4], Simiao Gong[1,2,3,4], Yuan Ma[1,2,3,4], Peiyan Han[1,2,3], Nan Wang[1,2,3], Zongheng Fu[1,2,3], Xinyi Zhang[1,2,3], Xinyang Huang[1,2,3], Tianyu Yang[1,2,3], Hanze Tong[1,2,3], Guang-Rong Zhao[1,2,3], Yi Wu[1,2,3] ✉ & Ying-Jin Yuan[1,2,3]

The site-specific recombination system is a versatile tool in genome engineering, enabling controlled DNA inversion or deletion at specific sites to generate genetic diversity. The multiplexed inversion system, which preferentially facilitates inversion at reverse-oriented sites rather than deletion at same-oriented sites, has not been found in eukaryotes. Here, we establish a multiplexed site-specific inversion system, Rci51-5/multi-*sfxa101*, in yeast. Firstly, we develop a high-throughput screening system based on the on/off transcriptional control of multiple markers by DNA inversion. After two rounds of progressively stringent directed evolution, a mutant Rci51-5 shows an ability of multisite inversion and a ~1000-fold increase in total inversion efficiency against the wild-type Rci derived from *Salmonella typhimurium*. Subsequently, we demonstrate that the Rci51-5/multi-*sfxa101* system exhibits significantly lower deletion rate than the Cre/multi-*loxP* system. Using the synthetic metabolic pathway of β-carotene as an example, we illustrate that the system can effectively facilitate promoter substitution in the metabolic pathway, resulting in a more than 7-fold increase in the yield of β-carotene. In summary, we develop a multiplexed site-specific inversion system in eukaryotes, providing an approach to metabolic engineering and a tool for eukaryotic genome manipulation.

The site-specific recombination system is a commonly used tool for genome manipulation, characterized by its specificity, high efficiency, and low off-target rate[1–3]. Recently, these systems have been applied in many areas, including crop improvement[4], cell lineage tracing[5,6] and metabolic engineering[7]. Recombinases catalyze site-specific recombination by attacking the DNA backbone to mediate double-strand exchanges and the process does not involve DNA synthesis, degradation, or cofactors such as ATP[8]. Site-specific recombination systems can generate deletion, inversion, or other structural variations between two specific sites by configuring the orientation and location of sites[9]. Multiplexed site-specific recombination systems can induce a large number of rearrangement events in a short time, thereby effectively expanding the diversity of structural variations[10]. However, existing eukaryotic multisite recombinases inevitably lead to undesired deletions of DNA fragments among sites when multiple sites coexist[11] (Fig. 1a). For instance, in the Sc2.0 project, researchers have developed a Synthetic Chromosome Rearrangement and Modification by *loxP*-mediated Evolution (SCRaMbLE) system, which can rapidly

[1]State Key Laboratory of Synthetic Biology, Tianjin University, Tianjin 300072, China. [2]Frontiers Science Center for Synthetic Biology and Key Laboratory of Systems Bioengineering (Ministry of Education), School of Chemical Engineering and Technology, Tianjin University, Tianjin 300072, China. [3]Frontiers Research Institute for Synthetic Biology, Tianjin University, Tianjin 300072, China. [4]These authors contributed equally: Jieyi Li, Simiao Gong, Yuan Ma. ✉e-mail: yi.wu@tju.edu.cn

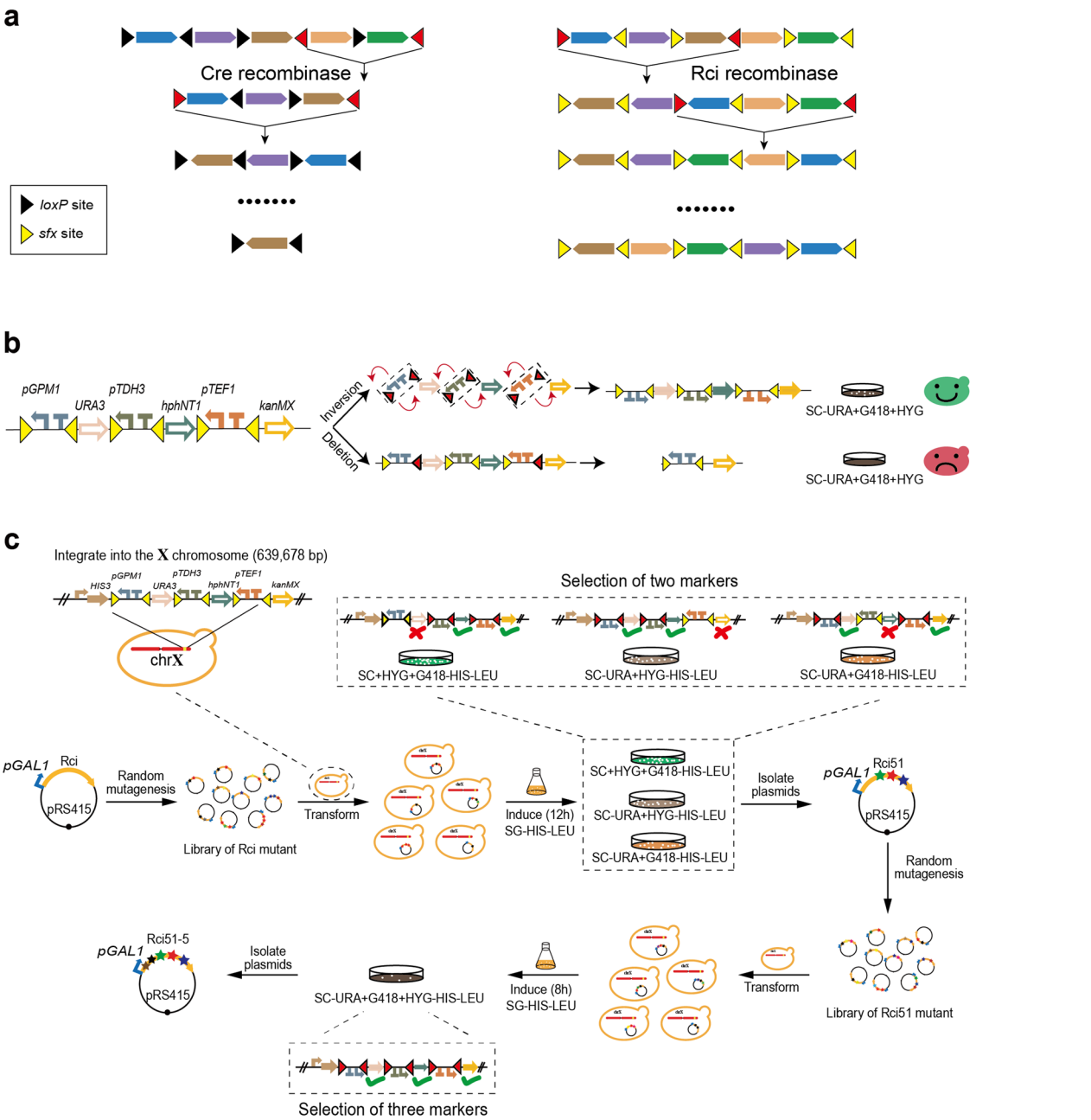

Fig. 1 | Concept and screening of a eukaryotic multiplexed site-specific inversion system. a Comparison of conventional tyrosine recombinase (Cre enzyme) and DNA inversion enzyme (Rci enzyme). Cre enzyme typically induces deletion of DNA fragments between directly repeated sites when multiple sites are present. The Rci enzyme facilitates gene inversion between reverse-oriented sites. The black and yellow triangles, respectively, represent the *loxP* site and the *sfx* site and the red triangles indicate the sites that mediate recombination. **b** High-throughput screening system for multiplexed site-specific inversion enzyme. The promoters and open reading frames (ORFs) are arranged alternately but in opposing orientations, with the combination of promoter and corresponding terminator situated between a pair of inverted *sfxa101* sites (yellow). Open arrows indicate silencing of selection markers, and solid arrows indicate expression of selection markers. The red triangles represent the sites that mediate recombination. **c** Flow diagram of two rounds of progressively stringent directed evolution in *Saccharomyces cerevisiae*. Fragment of the high-throughput screening system (7170 bp in length) was inserted into the chromosome X at the position of 639, 678 bp. The dashed line shows an example of the inversion situation of strains that can grow on the selective medium.

drive genome structural rearrangements by interactions among thousands of *loxPsym* sites inserted into the synthetic chromosomes of *Saccharomyces cerevisiae*[12–14]. Meanwhile, the insertion of *loxPsym* sites into the genome causes extensive deletions of essential genes during recombination, leading to strain lethality[15,16]. Applying the Cre/*loxP* system for cell barcoding involves the insertion of multiple *loxP* sites among the barcodes. Although the diversity of barcode can be generated through random recombination among these sites, it will gradually decrease over time due to deletions between same-oriented sites[5]. DNA inversion system, a site-specific recombination system in bacteria, prefers inversions at reverse-oriented sites rather than deletions at same-oriented sites when multiple sites coexist[17–19]. However, our previous research indicates that the prokaryotic inversion system does not work in eukaryotes, and the multiplexed site-specific inversion system has not been found in eukaryotes[20].

In this study, we establish a multiplexed site-specific inversion system Rci51-5/multi-*sfxa101* in eukaryotes that preferentially facilitates inversion at reverse-oriented sites rather than deletion at same-

oriented sites. The mutant Rci51-5, with a ~1000-fold increase in total inversion efficiency against the wild-type, is obtained through a high-throughput screening strategy following two rounds of progressively stringent directed evolution. Five nonsynonymous mutations of Rci51-5 have been found to synergistically contribute to the enhanced efficiency of inversion. Our system of Rci51-5/multi-*sfxa101* shows a significantly lower deletion rate than the Cre/multi-*loxP* system. We demonstrate the application of the Rci51-5/multi-*sfxa101* system for optimizing the metabolic pathways of multiple genes by promoter substitution between an array of varied strength promoters and multiple genes of synthetic pathways. Using the biosynthetic pathway of β-carotene as an example, upon the Rci51-5 expression, the original promoters of exogenous genes are replaced by promoters in the array, leading to changes in transcriptional levels and improvement of β-carotene production. In conclusion, this eukaryotic multiplexed site-specific inversion system enriches the types of eukaryotic site-specific recombination systems and offers a special tool for genome engineering.

Results

Developing a high-throughput screening system for multiplexed site-specific inversion enzyme

The site-specific DNA inversion system is biased for DNA inversion and has previously been exclusively identified in prokaryotes[17,21–23]. In earlier studies, utilizing the wild-type Rci enzyme from *Salmonella typhimurium* and directed evolution, we have developed a DNA inversion system (Rci8/*sfxa101*) in eukaryotes, working at a pair of recombination sites[20]. To test whether this mutant (Rci8) can accomplish multisite inversion, we developed a screening system of multisite inversion in *Saccharomyces cerevisiae* (Fig. 1b). The system comprises three promoters − *pGPM1*, *pTDH3*, *pTEF1* and corresponding terminators, along with three open reading frames (ORFs) that can be used for auxotroph or resistance screening − *URA3*, *hphNT1* and *kanMX*. The promoters and ORFs are arranged alternately in opposing orientations, with inverted *sfxa101* inversion sites inserted at both ends of each promoter-terminator pair. Upon inducing enzyme expression, inversions among the *sfxa101* sites regulate on/off transcription of the selection markers, enabling yeast growth on corresponding selective media. To ensure stability, we integrated the sequence of the screening system into the X chromosome of *Saccharomyces cerevisiae*. Using the screening system of DNA inversion enzyme, we tested the multisite inversion capabilities of the wild-type Rci and the mutant Rci8. After 12 h of induced expression, yeast colonies containing the wild-type Rci or Rci8 can only grow on media of a single selection but not on media of two or three selections, indicating that neither enzyme could efficiently mediate multisite inversion (Supplemental Fig. 1).

Establishing a eukaryotic multiplexed site-specific inversion system through two rounds of progressively stringent directed evolution

Directed evolution is a regular approach for generating mutants and selecting desirable functions, which has become a powerful technology platform in protein engineering[24,25]. We expect to enhance the multisite inversion efficiency of the Rci enzyme through directed evolution and the high-throughput screening system for multiplexed site-specific inversion enzymes (Fig. 1c). Error-prone PCR was used to introduce random mutations into the coding sequence of wild-type Rci[26]. The plasmid libraries of mutants were transformed into the yeast strain *yLJY001*, which contained the screening system. Firstly, we plated the induced yeast on media of two selections (SC-URA+HYG-HIS-LEU, SC+HYG+G418-HIS-LEU, SC-URA+G418-HIS-LEU) to screen mutants capable of multisite inversion. In this round of directed evolution, 109 unique mutants were identified by Sanger sequencing and 12 mutants with a total inversion efficiency of over 0.1% were selected. The mutant Rci51 shows the highest total inversion efficiency up to 10.8%, which is a ~350-fold improvement compared with the wild-type, although the co-inversion efficiency of three markers remains low (Fig. 2a, b). To further improve multisite inversion efficiency, Rci51 was chosen as a template for a second round of directed evolution with increased selection pressure through a shorter induction time and three selection markers. Cells with the library of Rci51 mutants were induced for 8 h and plated on a medium of three selections (SC-URA+G418+HYG-HIS-LEU). After this second round, we identified 23 unique mutants, among which three were superior to Rci51 in both total inversion efficiency and three-markers co-inversion efficiency. Specifically, the mutant Rci51-5 shows the highest co-inversion efficiency of three markers, and the total inversion efficiency reaches 35.9% (Fig. 2a, b). To visually characterize the efficiency of multisite inversion for the wild-type Rci, Rci51, and Rci51-5, the induced yeast cells were plated on various selective media at the same concentration. The results show that Rci51-5 could generate a greater number of inverted colonies than wild-type Rci and Rci51 under various selective conditions (Fig. 2c). Especially, hundreds of clones containing Rci51-5 could grow on the media with three co-inversion selections, whereas almost none clones grew for Rci and Rci51. We also tried a third round of directed evolution, unfortunately, we did not obtain mutants with efficiency and specificity of multisite inversion higher than Rci51-5 (Supplemental Fig. 2).

To compare the efficiency of Rci51-5 at different inversion sites, we tested the inversion efficiency of the Rci51-5 at *sfxa101*, *sfxa102*, *sfxa107*, *sfxa108*, *sfxa109*, *sfxa112*[27]. The result indicated that the *sfxa101* site shows the highest efficiency among the *sfx* recombination sites (Supplemental Fig. 3), which is consistent with results in bacteria[27–29]. Therefore, a multiplexed inversion system was established in yeast based on the inversion enzyme Rci51-5 and *sfxa101* sites. Furthermore, by constructing a double fluorescence detection system, we preliminarily verified that the system of Rci51-5/multi-*sfxa101* could work in HEK-293T cells (Supplemental Fig. 4). In addition, the wild-type Rci enzyme belongs to the tyrosine recombinase family and we tested the orthogonality of the Rci51-5/*sfxa101* system against the commonly utilized site-specific recombination systems (Cre/*loxP*[30], Flp/*frt*[31], and Vika/*vox*[32]). The results showed that Rci51-5 was exclusively active at the *sfxa101* site, while other recombinases exhibited no activity at the *sfxa101* site (Supplemental Fig. 5), indicating that the Rci51-5/*sfxa101* system is orthogonal to those above site-specific recombination systems. To improve the robustness of the system, we used a genetic AND gate[15] to achieve a tighter regulation of Rci51-5 expression, and integrated the transcriptional unit of Rci51-5 into the yeast genome (Supplemental Figs. 6, 7).

Synergistic effect of five mutations for the improved inversion efficiency of the evolved enzyme

To clarify the mutations of Rci51-5, we sequenced the full-length of Rci51-5 plasmid and the result of Sanger sequencing indicates the presence of five nonsynonymous mutations: Q30K, L109P, F246V, A295S and A330T (Fig. 2d). To determine which of these mutations or their combinations contributed to the enhanced inversion efficiency of Rci51-5, we constructed 23 mutants, each containing single mutation or various combinations of mutations. Then, we tested the multisite inversion efficiency of these mutants. The results from a single mutations demonstrated that only the F246V mutation could facilitate multisite inversion, with an efficiency of 0.021 relative to the Rci51-5, while others could not (Fig. 2e). In the combination of two mutations, the efficiency of the L109P & F246V increases by 15-fold compared to the F246V mutation. Some combinations of three or four mutations (Q30K & L109P & F246V, Q30K & L109P & F246V & A295S) can further improve the efficiency of inversion, while others show a decrease in inversion efficiency. A similar phenomenon has also been observed in other protein engineering studies of multi-mutational variants[33,34]. The multisite inversion efficiency of the Rci51-5 mutant, which contains five

https://doi.org/10.1038/s41467-025-57206-w

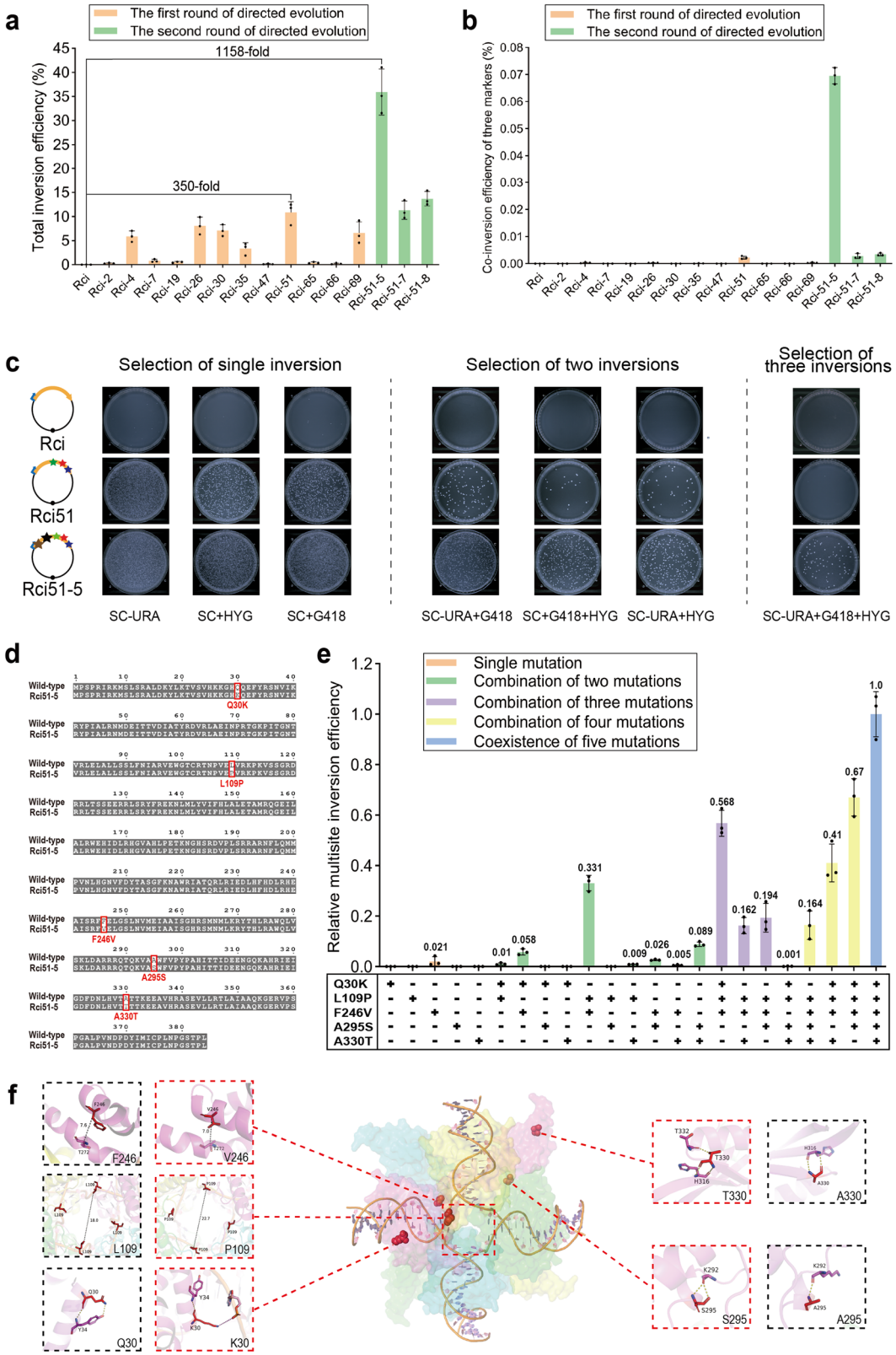

mutations, is higher than all other mutants. We then employed the AlphaFold3 to predict structure of the protein-nucleic acid complex of Rci51-5/*sfxa101* for visualization[35] (Fig. 2f). The precited structure of Rci51-5/*sfxa101* exhibits a tetrameric complex structure, similar to the structure of Cre/*loxP*[36]. By closely looking at the predicted structure, we observed that the F246V may reduce the steric hindrance, leading to a closer proximity of the two helices in the middle of the protein chain, and mutants containing the L109P show a tendency to expand central channel of the tetrameric complex. These are likely important for the efficient formation of tetrameric complex of the Rci enzyme, which may account for the significant improvement in efficiency for the combination of L109P & F246V. In addition, the other three mutants are found to potentially exhibit additional interactions in the complex of tetrameric-DNA (a salt bridge of protein-DNA for K30, new

Fig. 2 | The outcome of two rounds of progressively stringent directed evolution and mutations analysis. a The total inversion efficiency of the mutants generated in the two rounds of directed evolution. The orange and green represent the mutants produced in the first and second rounds of directed evolution, respectively. The error bars represent standard deviation of three biological replicates. **b** The co-inversion efficiency of three markers for the mutants generated during the two rounds of directed evolution. The efficiency is calculated following 12 h of induction. The orange and green represent the mutants produced in the first and second rounds of directed evolution, respectively. The error bars represent standard deviation of three biological replicates. **c** Yeast colonies containing the wild-type Rci, Rci51, or Rci51-5 were grown on various selective media after inducing 12 h, respectively. Compared to the Rci and Rci51, more colonies of Rci51-5 were grown on selective media as the number of selection markers increased. The pictures were taken after 3 days incubation at 30 °C. **d** Sequence alignment of Rci51-5 and the wild-type Rci. The mutant Rci51-5 identified five nonsynonymous mutations (red rectangle). **e** The relative multisite inversion efficiency of mutants containing single or combinations of mutations. '+' indicates the introduction of specific mutations in Rci sequence; '-' indicates their absence. The error bars represent standard deviation of three biological replicates. **f** Structural details of the inversion enzyme/DNA system by AlphaFold3. Two *sfxa101* DNA(s) are shown in the protein-nucleic acid complex with four Rci51-5 monomers (the four are in blue, green, yellow and magenta cartoon, respectively). Mutation residues are depicted in spheres. The dashed box marks the region zoomed in and showed in detail (Rci51-5 and the wild-type Rci are in red and black, respectively). The hydrogen bonds and salt bridges are depicted with yellow and magenta dashed lines, respectively. Source data for this figure are provided as a Source Data file.

hydrogen bonds for S295 and T330). Previous studies have shown that the change of amino acid residues for nucleases is related to the protein activity conformation and protein anchoring ability to DNA[37]. We speculate that these five nonsynonymous mutations may synergistically affect the interaction of tetrameric Rci51-5 and DNA molecules, thus improving recombination efficiency, although it is still difficult to reveal the explicit mechanism of the synergistic effects for five mutations especially in the in vivo environment of yeast cells[34].

Rci51-5/multi-*sfxa101* system shows a lower rate of deletion than Cre/multi-*loxP* system

The Cre/*loxP* system is one of the most widely used site-specific recombination systems, which can efficiently mediate the deletion between same-oriented sites or inversion between reverse-oriented sites without accessory proteins[30]. However, when applying the Cre/*loxP* system at multiple sites, such as in cell barcoding construction[5] and metabolic pathway optimization[7], deletions may result in decreased library diversity and loss of the targeted genes. The multiplexed site-specific inversion system we developed in eukaryotes may provide a tool to address this issue. To compare the Rci51-5/multi-*sfxa101* with the Cre/multi-*loxP* systems, we constructed two circuits containing multiple *sfxa101* and *loxP* sites, respectively. The circuits also contain a metabolic pathway capable of generating color compounds, enabling the rapid verification of recombination outcomes. We assembled an array containing ten promoters and corresponding terminators and selected three transcription units involved in the β-carotene pathway. The array and the transcription units are oriented in opposing directions, with the *sfxa101* or the *loxP* sites inserted into 3′ of promoters, respectively (Fig. 3a). The deletion events mediated by recombinase might disrupt the metabolic pathway, leading to the appearance of white yeast colonies[38]. The induced yeast containing the Rci51-5/multi-*sfxa101* or Cre/multi-*loxP* were plated and the proportion of white colonies was counted at different times. At 24 h, the number of white colonies in the Cre/multi-*loxP* system is significantly higher compared to the Rci51-5/multi-*sfxa101* system (Fig. 3b). Within 48 h, the proportion of white colonies for the Rci51-5/multi-*sfxa101* system is notably lower than the Cre/multi-*loxP* system, although it increases slowly over time (Fig. 3c). The results showed that the deletion rate of the Rci51-5/multi-*sfxa101* system was notably lower than Cre/multi-*loxP*. Furthermore, we counted the proportions of dark orange colonies for two systems at various time points. Within 48 h, the numbers of dark orange colonies for Rci51-5/multi-*sfxa101* system increased over time, whereas the Cre/multi-*loxP* system demonstrated a decline after 24 h, which was most likely attributed to the accumulation of deletions (Supplemental Fig. 8).

Applying multiplexed site-specific inversion system to promoter substitution for metabolic engineering

In the field of metabolic engineering, the production of target compounds involves the co-expression of multiple genes along a metabolic pathway[39,40]. Identifying the optimal combination of gene expression levels is crucial for increasing the yield of target products, and promoter engineering is an important tool in achieving this goal[41–43]. By inserting recombination sites among promoters of varying strengths and exogenous genes, respectively, site-specific recombination systems can be utilized for metabolic engineering by generating new transcriptional combinations. The multiplexed site-specific inversion system we developed exhibits a bias for inversions rather than deletions, which decreases the risk of loss of exogenous genes, giving it a unique advantage in constructing multi-gene promoter regulation systems for metabolic pathways.

Taking the biosynthetic pathway of β-carotene as an example, we applied the multiplexed site-specific inversion system to promoter engineering and evaluated the substitution of promoters via a PCR-based rapid verification strategy (Fig. 4a). This strategy confirms whether the original promoters of exogenous genes have been replaced and identifies which promoters have replaced them. The diversity of promoter substitution can be assessed through mixed colonies PCR. The yeast culture induced for 24 h in a liquid medium served as the mixed template for PCR, while the uninduced *yLJY023* was the control. For each exogenous gene, forward primers (F-crtYB, F-crtI, F-crtE) are combined with the reverse primers of their original promoters (R-1, R-2, R-3), as well as with primers F1-F10 for the ten promoters in the array, and a total of 33 PCR assays are conducted. The results of PCR showed that for each exogenous gene, all 11 primer pairs in the mixed template yielded positive bands, while in the control, only the primers of exogenous genes and the primers of original promoters could amplify positive bands. These findings demonstrate that in the experimental group, original promoters of exogenous genes could be replaced by any promoter from the array (Fig. 4b). To characterize the efficiency of promoter substitution, yeast cultures were plated at various induction times, and 256 single clones were randomly selected and validated using PCR to confirm the substitution of the original promoters. The results showed that the efficiency of promoter substitution improved with increasing induction time (Fig. 4c). At 48 h, the proportions of yeasts with one, two, and three promoters replaced are 44%, 8.1%, and 4.0%, respectively, and the total efficiency of promoter substitution is up to 56.1%. In order to assess the stability of the system, we performed a 14 day consecutive subculturing of the strain *yLJY023*, which harbors the plasmid of multiplexed site-specific inversion system (Supplemental Fig. 9a). The results of PCR and whole genome sequencing confirmed the long-term stability and capability of the Rci51-5/multi-*sfxa101* system (Supplemental Fig. 9b, c).

Next, we evaluated the ability of the multiplexed site-specific inversion system to diversify gene transcription and boost production of β-carotene in metabolic pathways. The synthesis of β-carotene involves multiple genes (Fig. 4d) and our previous research has demonstrated a correlation between phenotypic color and carotenoid yield in yeast[38]. In this study, we selected colonies with various colors and identified 11 strains with unique combinations of exogenous genes and promoters by PCR. Through a systematic analysis of genotypes and production of carotenoids for all

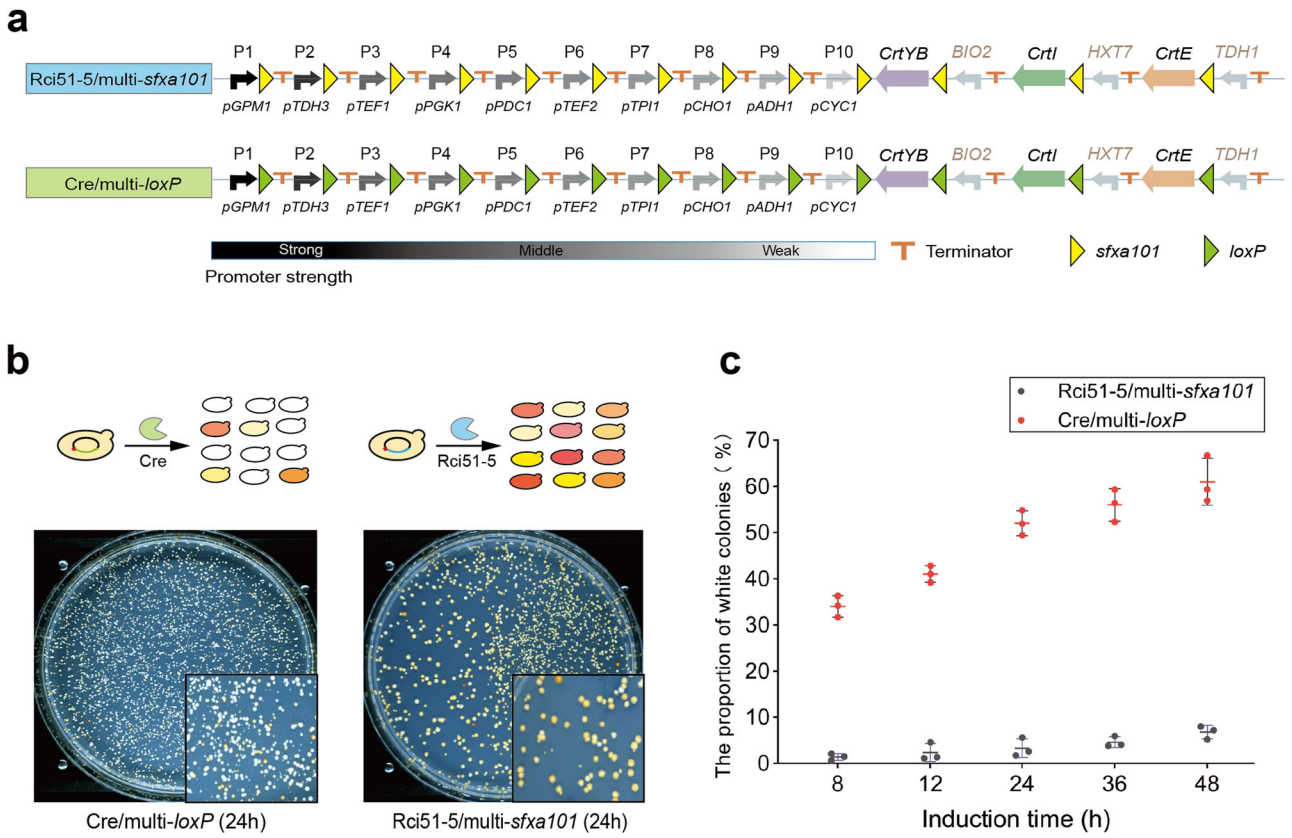

Fig. 3 | Comparison of the Rci51-5/multi-*sfxa101* system and Cre/multi-*loxP* system. a Two circuits design to validate the recombination outcome of different systems. The 3′ and 5′ of the circuit consist of the promoter array and exogenous genes, respectively. The recombination site is inserted into 3′ of each promoter. The promoter array encompasses a range of promoters with different strengths (color scale): strong promoters *pGMP1*, *pTDH3*, *pTEF1*, medium-strength promoters *pPGK1*, *pPDC1*, *pTEF2*, *pTPI1*, and weak promoters *pCHO1*, *pADH1*, *pCYC1*. The yellow triangles represent the *sfxa101* site, while the green triangles represent the *loxP* site. **b** Yeast colonies induced by different recombination systems. The magnified region shows different colony colors and the white colonies of the Rci51-5/multi-*sfxa101* system are significantly lower than the Cre/multi-*loxP* system. The cultures induced by 24 h were spread on synthetic complete medium lacking leucine and uracil (SC-Leu-Ura). The pictures were taken after 7 days incubation at 30 °C. **c** The proportion of white colonies to total colonies at different induction times. Bars and error bars represent average and standard deviation of three biological replicates, respectively. Source data for this figure are provided as a Source Data file.

tested strains, we found that strains with enhanced transcription of the *crtI* (*yLJY045* and *yLJY028*) or *crtYB* (*yLJY044* and *yLJY055*) showed a 4.9–6.3 fold-change and 1.9–2.6 fold-change for the production of β-carotene, respectively. The strain *yLJY045* increased the production of β-carotene with a 6.3-fold (1.16 μg/mg DCW) compared to the control *yLJY023*, with its original promoter *pHXT7* of *crtI* replaced by a strong promoter *pTDH3*. The qPCR results indicate a significant enhancement in the expression of the *crtI* gene for *yLJY045* (Fig. 4e). This result confirms that *crtI* is a rate-limiting enzyme for the biosynthetic pathway of β-carotene in *Saccharomyces cerevisiae*, as compared to *crtYB* and *crtE*, which is consistent with previous studies[44,45]. Moreover, strain *yLJY081* exhibits three inversions, in which original promoters of all exogenous genes have been replaced, resulting in a deep orange colony color. The results of high-performance liquid chromatography (HPLC) showed that the production of β-carotene and lycopene for *yLJY081* is 1.4 and 0.32 μg/mg DCW, corresponding to a 7.6-fold and 12.4-fold increase in yield compared to the original construct. Our result demonstrates that the multiplexed site-specific inversion system can be used to optimize gene expression for metabolic engineering. We also applied the multiplexed site-specific inversion system to the biosynthetic pathway of violacein (Supplemental Fig. 10).

Discussion

The multiplexed site-specific inversion system produces complex DNA rearrangements through random inversions among multiple sites, which plays a crucial role in generating genetic diversity and phenotypic adaptation[17,46,47]. Here, we developed a multiplexed site-specific inversion system in yeast based on Rci51-5 and *sfxa101* sites, which can manipulate gene inversions among multiple reverse-oriented sites and shows a significantly lower deletion rate than Cre/multi-*loxP*. Traditional approaches for altering gene expression profiles of metabolic pathways generally involve multiple rounds of combinatorial assembly[48–50], whereas our system only requires a simple initial one-step assembly process to generate a diverse library of cells upon the induction of inversion enzyme. Kevin et al. established GEMbLeR (multiplexed Gene Expression Modification by LoxPsym Cre Recombination), facilitating promoter/terminator substitution in *Saccharomyces cerevisiae* for the rapid optimizing of heterologous biosynthetic pathways[7]. Comparing with Cre/multi-*loxP* system, our Rci51-5/multi-*sfxa101* system could reduce the rate of deletions when applied to multi-gene optimization of metabolic pathways, and this advantage can be further expanded when applied to multiple rounds of metabolic engineering. In addition, the generation of diverse library of transcriptional combinations poses additional challenges for downstream high-throughput screening. In this study, we rely on phenotypic color-based screening, while it is not applicable to the screening of colorless products. Other advanced high-throughput screening methods[51,52], such as the combination of transcription factor-based biosensors and fluorescence-activated cell sorting (FACS), have the potential to expand the application of our system to broader metabolic productions. In

https://doi.org/10.1038/s41467-025-57206-w

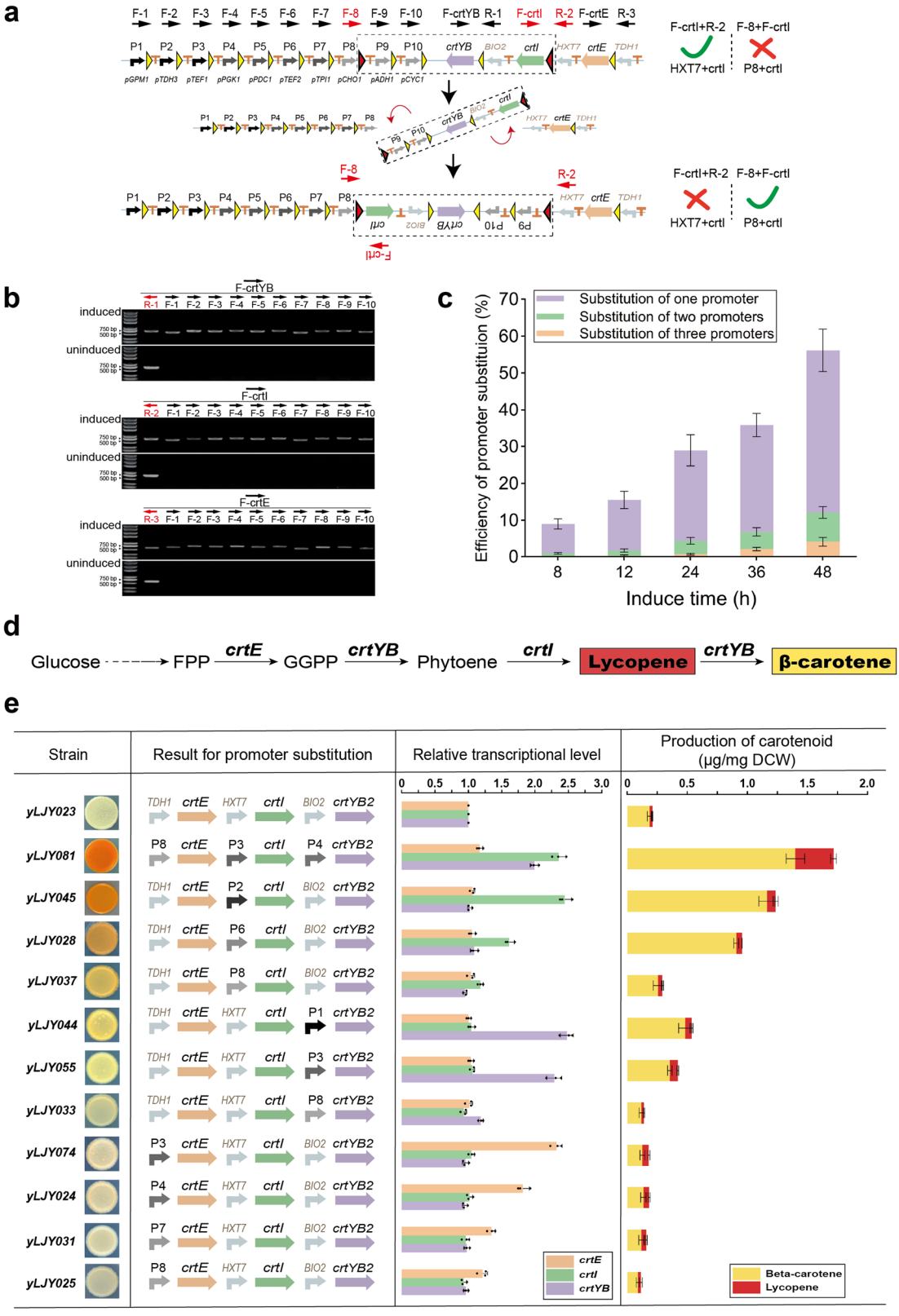

the multi-gene promoter regulation system, the original promoter of *crtYB* is more easily substituted, potentially indicating a positional preference among multiple inversion sites (Supplemental Fig. 11). A feature of the multiplexed site-specific inversion system is to change the relative position of DNA through inversion, and it may have the capacity to address this issue by iterative rounds of inversion.

Although the rate of deletion for the Rci51-5/multi-*sfxa101* system is notably lower than the Cre/multi-*loxP* system, instances of deletion leakage have been detected in our study. In the future, the system might be further optimized in terms of recombinases, recombination sites, and co-factors: (1) The AI-assisted rational design of enzymes might accelerate the acquisition of recombinases with lower deletion rate[53]; (2) The sequence of the *sfx* can affect the inversion frequency

Fig. 4 | The multiplexed site-specific inversion system applied to promoter substitution for metabolic engineering. a Schematic diagram of PCR strategy for validating whether the original promoter has been replaced. The horizontal arrows indicate the orientation of primers. The promoters P1-P10 consist of *pGPM1*, *pTDH3*, *pTEF1*, *pPGK1*, *pPDC1*, *pTEF2*, *pTPI1*, *pCHO1*, *pADH1* and *pCYC1*. Taking the original promoter *pHXT7* of *crtI* is replaced by promoter P8 as an example to illustrate the verification strategy: when P8 replaces *pHXT7*, the forward primer F-crtI becomes a reverse primer, which can amplify a short positive band with F-8 (green '√') through PCR reaction, whereas F-crtI and R-2 can not (red '×'). **b** Three sets of PCR results for mixed colonies. The top, middle, and bottom panels show the PCR results of primer of *crtYB*, *crtI*, *crtE* with the primers of promoters (one primer of original promoter, ten primers of promoters in the array), respectively. The top of each set of gel represents the experimental group (induced liquid cultures) and the bottom represents the control (uninduced liquid cultures). The detailed sequence of primers is shown in Supplemental Table 3. **c** The efficiency of promoter substitution. The error bars represent standard deviation of three biological replicates. **d** β-carotene biosynthesis pathway in *Saccharomyces cerevisiae*. Bold characters on the arrows represent exogenous genes targeted for expression optimization. Full/dashed arrows indicate one/multiple enzymatic conversion(s). **e** The multi-gene promoter regulation system for β-carotene pathway. The correlation among genotype, production of carotenoid and the expression levels of exogenous genes in strains with replaced original promoters. The control *yLJY023* is not induced, and other strains are arranged in descending order based on color intensity. The results for exogenous gene promoter substitution are verified by PCR analysis. The transcriptional levels of exogenous genes are evaluated by qPCR (the transcriptional levels of three exogenous genes in the control *yLJY023* are set as the base value). The error bars represent standard deviation of three biological replicates. The yields of carotenoid are determined by high-performance liquid chromatography (HPLC). Quantification is performed in biological triplicate for each strain as shown. The error bars represent standard deviation of three biological replicates. Source data for this figure are provided as a Source Data file.

and specificity[27] and the design and modification of the sequence of the *sfx* site might facilitate the inversion events; (3) The specificity of the system may be further optimized by introducing factors, such as nucleoid-associated protein HU and nucleoid protein Fis (Factor for inversion stimulation)[17]. In addition, when applied the multiplexed site-specific inversion system to metabolic engineering, incorporating a backup pathway may eliminate the risks caused by the deletion events. While we have shown that the inversion system is stable within a period of time, for a longer-term stability in the application of industrial-scale production, we suggest that removing the inversion system after determining the desired mutant.

The promoters of varying types and transcriptional strength derived from promoter engineering[54,55] can be incorporated into the multiplexed site-specific inversion system to promoter substitution, which holds the potential to generate more diverse combinations of gene expression. Moreover, many other metabolic engineering strategies might be combined with our system to further enhance the productivity of useful chemicals[56–59]. Based on the capability of the Rci51-5/multi-*sfxa101* system to invert at multiple sites in HEK-293T cells, it offers potential applications in constructing cellular barcodes and genetic circuits, providing an alternative to the Cre/multi-*loxP* system[5,60,61]. As the system is orthogonal to other commonly used site-specific recombination systems, it can be combined with other systems to enhance the scale and flexibility when manipulating larger-scale complex gene rearrangements.

In conclusion, we have developed a multiplexed site-specific inversion system capable of inducing DNA inversions among multiple sites in eukaryotes. This system provides an approach to altering multiplexed gene expression for metabolic engineering and a unique tool for genome engineering in eukaryotes.

Methods

Strains, plasmids, and growth medium

The yeast strains and plasmids used in this study are listed in Supplemental Tables 1 and 2, respectively. Yeast strains were grown at 30 °C in YPD medium (20 g/L glucose, 20 g/L peptone, 10 g/L yeast extract). For selective growth, the plasmid-harboring yeast strains were cultured in Synthetic Complete (SC) medium supplemented with a 2 g/L dropout mixture lacking leucine, histidine, tryptophan, and uracil, with additional components added according to selective requirements. Liquid culture was grown at 30 °C and 220 rpm in incubator. Expression of Rci mutants, regulated by the inducible promoter *GAL1*, was induced in SC medium containing 2% galactose. For Cre recombinase, fusion with an Estrogen Binding Domain (EBD) enabled estradiol-dependent regulation, with induction achieved using SC medium supplemented with 1 μM β-estradiol. Modified SC medium included SC+GAL (20 g/L galactose replacing glucose), SC+EST (1 μM β-estradiol), SC+HYG (0.3 g/L hygromycin), and SC+G418 (1 g/L geneticin). *Escherichia coli* Trans-T1 (Beijing Biomed Co., Ltd.) was used for plasmid transformation. *Escherichia coli* was grown at 37 °C in LB medium (15 g/L agar, 10 g/L tryptone, 5 g/L yeast extract, 10 g/L NaCl). 100 mg/L ampicillin or kanamycin was added for selection. The sequence of the screen system was integrated into the right arm of X chromosome in yeast by homologous recombination[62].

Construction of mutant library

Random mutations were introduced into the Rci encoding sequence via error-prone PCR, generating a library of 1.0×10^7 unique colonies with 1–4 mutations per kb in the Rci gene[26]. The library capacity and mutation frequency in the second and third rounds of directed evolution were the same as in the first round, using Rci51 and Rci51-5 as templates for mutagenesis, respectively. The Rci mutant library was constructed and tested following the standard protocol of GENEWIZ, and the sample was sent on dry ice to GENEWIZ, Suzhou.

Selection of multiplexed site-specific inversion enzyme

The library of mutant plasmid was introduced into *yLJY001*, which contains the screening system for multiplexed site-specific inversion enzyme[63]. The gene of Rci variants was cloned on a centromeric plasmid and transcriptionally controlled by an inducible promoter *GAL1*. The transformed strains were cultured in a liquid medium (SC-HIS-LEU +GAL) for 12 h. Induced yeast cells were plated in triplicate on media (SC+HYG+G418-HIS-LEU, SC-URA+HYG-HIS-LEU, SC-URA+G418-HIS-LEU) to screen for mutants that underwent multisite inversion. Strain colonies capable of growing on media of two selections were selected for yeast plasmid extraction, followed by enrichment of plasmids containing Rci mutants through *E. coli* transformation[64]. The mutation sites of the enzyme were determined by Sanger sequencing. During the second round of directed evolution, yeast transformation and induction culture are the same as the first round, but the induction time of Rci51 mutants is reduced from 12 h to 8 h. The induced cells are directly plated on SC-HIS-LEU-URA+G418+HYG to increase the selection pressure (Fig. 1c).

In the third round of directed evolution, the mutant plasmid library of Rci51-5 was transformed into yeast strains containing a specific screening system for the inversion enzyme by *Saccharomyces cerevisiae* lithium acetate transformation[63]. The transformed cells were cultured in a liquid medium (SC-LEU+HYG+GAL) for 12 h. The induced yeast cells were spread on SC-URA-LEU+HYG to screen for mutants undergoing inversion reaction. A total of 5000 mutants were randomly selected and replicated on SC-HIS-LEU+HYG+GAL medium to assess deletion efficiency. Among them, mutants that can barely grow on SC-HIS-LEU+HYG+GAL medium were selected, indicating inversion capability with decreased deletion efficiency. The plasmids containing Rci51-5 mutations were extracted and enriched[64]. These plasmids were then transformed into yeast strain *yLJY001* to validate the efficiency of

multisite inversion. Mutant plasmids capable of growing on SC-URA +G418+HYG-HIS-LEU after induction expression with galactose for 12 h were selected for sequencing verification (Supplemental Table 2).

Inversion efficiency assay for Rci mutants

To test the inversion efficiency of mutants, yeasts carrying the Rci mutants were individually plated on media of one, two, or three selections and medium without selections. We defined the total inversion efficiency as the ratio of colonies on media of a single selection (SC-URA-HIS-LEU, SC+G418-HIS-LEU, SC+HYG-HIS-LEU) to those on medium without selection. The efficiency of co-inversion three markers was defined as the ratio of colonies on the medium of three selections (SC-URA+G418+HYG-HIS-LEU) to those on the medium without selection.

Inversion efficiency assay for different *sfx* sites

The different *sfx* sites (*sfxa101*, *sfxa102*, *sfxa107*, *sfxa108*, *sfxa109*, *sfxa112*) were cloned into the recombination reporter vectors. Plasmids containing different *sfx* sites were introduced separately into yeast that contained the plasmid of the Rci51-5[63]. The transformed strains were cultured in a liquid medium (SC-HIS-LEU+GAL) for 12 h, and the induced yeast cells were plated in triplicate on SC-URA-HIS-LEU and SC-HIS-LEU. The inversion efficiency is the ratio of colonies on SC-URA-HIS-LEU to those on SC-HIS-LEU.

Orthogonality of the Rci51-5/*sfxa101* system assay

The *sfx* sites in Supplemental Fig. 3a were replaced with *vox*, *frt*, or *loxP* sites, respectively. Plasmids containing different recombination sites were introduced separately into yeast that contained the plasmid of the Rci51-5. The transformed strains were cultured in a liquid medium (SC-HIS-LEU+GAL) for 12 h. Induced yeast cells were plated in triplicate on SC-URA-HIS-LEU. The plasmids containing Cre, Flp and Vike recombinase expression genes were introduced separately into yeast containing the recombinant reporter vector containing *sfxa101* sites. Induced different recombinant enzymes for 12 h and induced yeast cells were plated medium with URA selection, respectively.

Cell culture, plasmid transfection, and fluorescence microscopy

HEK-293T cells (ATCC) were cultured in Dulbecco's modified Eagle's medium (DMEM) (Procell) supplemented with 10% FBS (Procell) at 37 °C with 5% CO_2. For plasmid transfection, 293T cells were seeded in 6-well plates (Corning) at 70% confluence. Transfection was performed by mixing 5 μg of plasmid with 250 μL of Opti-MEM (Gibco) and 7 μL of Liposomal Transfection Reagent (Yeasen) with 250 μL of Opti-MEM (Gibco) separately for 5 min. The two solutions were thoroughly mixed and incubated at room temperature for 20 min, then the final mixture was added dropwise into each well of the 6-well plate. Cells were imaged at 48 h post-transfection using the EVOS M7000 live-cell fluorescence imaging system equipped with a fluorescence microscope.

Molecular modeling and structural analysis for protein-nucleic acid complexes

The three-dimensional structure model of the Rci, Rci51 and Rci51-5 were constructed based on their amino acid sequence using the AlphaFold3 program with default settings, and the structural information of the protein-nucleic acid complexes was obtained[35]. PyMOL software (Delano, 2010) was used to analyze structures of the complexes[65].

Deletion rate assay

The *yLJY022* and *yLJY023*, which contain a multi-gene promoter regulation system for the β-carotene metabolic pathway using Cre/multi-*loxP* and Rci51-5/multi-*sfxa101* respectively, were cultured in SC-URA-LEU+GAL and SC-URA-LEU+EST liquid medium for 12 h. A new medium was replaced every 12 h, and samples were taken at 8 h, 12 h, 24 h, 36 h, and 48 h, respectively. The samples were streaked on SC-LEU-URA at different times to calculate the proportion of white colonies.

Mixed colonies PCR

The yeast *yLJY023* was cultured in SC-URA-LEU+GAL and SC-URA-LEU liquid medium for 24 h, respectively. The strains cultured in the two media were used as templates for PCR. Each promoter substitution of the exogenous gene was verified by 11 pairs of PCR primers. The first set of primers included the forward primer for the exogenous gene and the reverse primer for its original promoter, while the subsequent 10 sets consisted of the forward primer for the exogenous gene and the forward primer for promoters in the array. A total of 33 PCR reactions were conducted.

Promoter substitution efficiency assay

The *yLJY023* was cultured in SC-URA-LEU+GAL for 12 h. A new liquid medium SC-HIS-LEU+GAL was replaced every 12 h, and samples were taken at 8 h, 12 h, 24 h, 36 h, and 48 h and plated on SC-LEU-URA. Colonies on the medium were randomly picked to verify the original promoter substitutions of *crtE*, *crtI*, and *crtYB* by the strategy described in Fig. 4a.

HPLC measurement of carotenoid production

The induced and control yeast strains were cultured in 5 mL of SC-Ura liquid medium at 220 rpm, 30 °C in a shaking incubator. The saturated cultures were diluted to an initial OD_{600} of 0.1 in 30 mL of SC-Ura liquid medium and grown for 72 h with the same condition. Cells from 10 mL culture were collected and then washed with double-distilled water and harvested by centrifugation, repeated twice. The cells were dried in a freeze dryer for measurement of the dry cell weight. The dry cells were resuspended in 700 μL of acetone and then shaken with quartz sand for 30 min. The acetone extracts were centrifuged and filtered with a 0.22 μm filter for subsequent analysis. The analysis of carotenoids was performed by HPLC (Waters 2695) equipped with BDS HYPERSIL C18 column (15 cm × 4.6 mm) and UV detection at 460-470 nm. The mobile phase consisted of acetonitrile-water (9:1 v/v) and methanol-2-propanol (3:2 v/v) with a flow rate of 1 mL per min at 25 °C. The content of the carotenoids was expressed as μg per mg dry cell weight. Each sample was performed on technical triplicates.

Statistics and reproducibility

All experiments included in this study were performed three times at least. All data are presented as mean ± standard deviation. No statistical method was used to predetermine sample size. No data were excluded from the analyses. The experiments were not randomized. The investigators were not blinded to allocation during experiments and outcome assessment.

Reporting summary

Further information on research design is available in the Nature Portfolio Reporting Summary linked to this article.

Data availability

All data supporting the findings of this study are available within the paper and its supplementary information files. Source data are provided with this paper.

References

1. Durrant, M. G. et al. Systematic discovery of recombinases for efficient integration of large DNA sequences into the human genome. *Nat. Biotechnol.* **41**, 488–499 (2023).
2. Kim, T., Weinberg, B., Wong, W. & Lu, T. K. Scalable recombinase-based gene expression cascades. *Nat. Commun.* **12**, 2711 (2021).

3. Vizoso, M. et al. A doxycycline- and light-inducible Cre recombinase mouse model for optogenetic genome editing. *Nat. Commun.* **13**, 6442 (2022).
4. Srivastava, V. G. D. Site-specific gene integration technologies for crop improvement. *Vitro Cell. Dev.l Biol. Plant* **46**, 219–232 (2010).
5. Pei, W. et al. Polylox barcoding reveals haematopoietic stem cell fates realized in vivo. *Nature* **548**, 456 (2017).
6. Liu, K., Jin, H. & Zhou, B. Genetic lineage tracing with multiple DNA recombinases: a user's guide for conducting more precise cell fate mapping studies. *J. Biol. Chem.* **295**, 6413–6424 (2020).
7. Cautereels, C. et al. Combinatorial optimization of gene expression through recombinase-mediated promoter and terminator shuffling in yeast. *Nat. Commun.* **15**, 1112 (2024).
8. West, S. C. Enzymes and molecular mechanisms of genetic recombination. *Annu. Rev. Biochem.* **61**, 603–640 (1992).
9. Meinke, G. et al. Cre recombinase and other Tyrosine recombinases. *Chem. Rev.* **116**, 12785–12820 (2016).
10. Zhou, S., Wu, Y., Xie, Z., Jia, B. & Yuan, Y. Directed genome evolution driven by structural rearrangement techniques. *Chem. Soc. Rev.* **50**, 11287–12788 (2021).
11. Tian, X. & Zhou, B. Strategies for site-specific recombination with high efficiency and precise spatiotemporal resolution. *J. Biol. Chem.* **296**, 100509 (2021).
12. Wu, Y. et al. Bug mapping and fitness testing of chemically synthesized chromosome X. *Science* **355**, eaaf4706 (2017).
13. Xie, Z. X. et al. Design and chemical synthesis of eukaryotic chromosomes. *Chem. Soc. Rev.* **46**, 7191–7207 (2017).
14. Richardson, S. M. et al. Design of a synthetic yeast genome. *Science* **355**, 1040–1044 (2017).
15. Jia, B. et al. Precise control of SCRaMbLE in synthetic haploid and diploid yeast. *Nat. Commun.* **9**, 1933 (2018).
16. Wang, J. et al. Ring synthetic chromosome V SCRaMbLE. *Nat. Commun.* **9**, 3783 (2018).
17. Johnson, R. C. Site-specific DNA inversion by serine recombinases. *Microbiol. Spectr.* **3**, 1–36 (2015).
18. Komano, T. Shufflons: multiple inversion systems and integrons. *Annu. Rev. Genet.* **33**, 171–191 (1999).
19. Kubo, A., Kusukawa, A. & Komano, T. Nucleotide sequence of the rci gene encoding shufflon-specific DNA recombinase in the IncI1 plasmid R64: homology to the site-specific recombinases of intergrase family. *Mol. General Genet. MGG* **213**, 30–35 (1988).
20. Han, P. et al. A DNA inversion system in Eukaryotes established via laboratory evolution. *ACS Synth. Biol.* **10**, 2222–2230 (2021).
21. Sandmeier, H., Iida, S. & Arber, W. DNA inversion regions Min of plasmid p15B and Cin of bacteriophage P1: evolution of bacteriophage tail fiber genes. *J. Bacteriol.***174**, 3936 (1992).
22. Plasterk, R. H., Ilmer, T. A. & Van de Putte, P. Site-specific recombination by Gin of bacteriophage Mu: inversions and deletions. *Virology* **127**, 24–36 (1983).
23. Moskowitz, I. P., Heichman, K. A. & Johnson, R. C. Alignment of recombination sites in Hin-mediated site-specific DNA recombination. *Genes Dev.* **5**, 1635–1645 (1991).
24. Packer, M. S. & Liu, D. R. Methods for the directed evolution of proteins. *Nat. Rev. Genetics* **16**, 379–394 (2015).
25. Romero, P. A. & Arnold, F. H. Exploring protein fitness landscapes by directed evolution. *Nat. Rev. Mol. Cell Biol.* **10**, 866–876 (2009).
26. Zaccolo, M., Williams, D. M., Brown, D. M. & Gherardi, E. An approach to random mutagenesis of DNA using mixtures of triphosphate derivatives of nucleoside analogues. *J. Mol. Biol.* **255**, 589–603 (1996).
27. Gyohda, A., Furuya, N., Kogure, N. & Komano, T. Sequence-specific and non-specific binding of the Rci protein to the asymmetric recombination sites of the R64 Shufflon. *J. Mol. Biol.* **318**, 975–983 (2002).
28. Gyohda, A., Zhu, S., Furuya, N. & Komano, T. Asymmetry of shufflon-specific recombination sites in plasmid R64 inhibits recombination between direct *sfx* sequences. *J. Biol. Chem.* **281**, 20772–20779 (2006).
29. Peikon, I., Gizatullina, D. & Zador, A. In *vivo* generation of DNA sequence diversity for cellular barcoding. *Nucleic Acids Res.* **42**, e127 (2014).
30. Austin, S., Ziese, M. & Sternberg, N. A novel role for site-specific recombination in maintenance of bacterial replicons. *Cell* **25**, 729–736 (1981).
31. Andrews, B. J., Proteau, G. A., Beatty, L. G. & Sadowski, P. D. The FLP recombinase of the 2 micron circle DNA of yeast: interaction with its target sequences. *Cell* **40**, 795–803 (1985).
32. Karimova, M. et al. Vika/vox, a novel efficient and specific Cre/*loxP*-like site-specific recombination system. *Nucleic Acids Res.* **41**, e37 (2012).
33. Nguyen, L. T. et al. Engineering highly thermostable Cas12b via de novo structural analyses for one-pot detection of nucleic acids. *Cell Rep. Med.* **4**, 101037 (2023).
34. Hollmann, F., Sanchis, N. & Reetz, M. Learning from protein engineering by deconvolution of multi-mutational variants. *Angew. Chem. Int. Edi.* **63**, e202404880 (2024).
35. Abramson, J. et al. Accurate structure prediction of biomolecular interactions with AlphaFold 3. *Nature* **630**, 493–500 (2024).
36. Kye, S., Andrews, N., Devante, P., Vickih, W. & Markp, F. Mechanisms of Cre recombinase synaptic complex assembly and activation illuminated by Cryo-EM. *Nucleic Acids Res.* **50**, 1753–1769 (2022).
37. Zhang, Y. et al. Catalytic-state structure and engineering of *Streptococcus thermophilus* Cas9. *Nat. Catal.* **3**, 813–823 (2020).
38. Wu, Y. et al. In *vitro* DNA SCRaMbLE. *Nat. Commun.* **9**, 1935 (2018).
39. Galanie, S. et al. Complete biosynthesis of opioids in yeast. *Science* **349**, 1095–1100, (2015).
40. Zhang, J. et al. A microbial supply chain for production of the anticancer drug vinblastine. *Nature* **609**, 341–347 (2022).
41. Mitchell, L. A. et al. Versatile genetic assembly system (VEGAS) to assemble pathways for expression in *Scerevisiae*. *Nucleic Acids Res.* **43**, 6620–6630 (2015).
42. Naseri, G. A roadmap to establish a comprehensive platform for sustainable manufacturing of natural products in yeast. *Nat. Commun.* **14**, 1916 (2023).
43. Smanski, M. J. et al. Functional optimization of gene clusters by combinatorial design and assembly. *Nat. Biotechnol.* **32**, 1241–1249 (2014).
44. Shi, B. et al. Systematic metabolic engineering of *Saccharomyces cerevisiae* for lycopene overproduction. *J. Agric. Food Chem.* **67**, 11148–11157 (2019).
45. Liang, N. et al. Exploring catalysis specificity of phytoene dehydrogenase *CrtI* in carotenoid synthesis. *ACS Synth. Biol.* **9**, 1753–1762 (2020).
46. Grindley, N., Whiteson, K. L. & Rice, P. A. Mechanisms of site-specific recombination. *Annu. Rev. Biochem.* **75**, 567–605 (2006).
47. Borst, P. & Greaves, D. Programmed gene rearrangements altering gene expression. *Science* **235**, 658–667 (1987).
48. Naseri, G., Behrend, J., Rieper, L. & Mueller-Roeber, B. COMPASS for rapid combinatorial optimization of biochemical pathways based on artificial transcription factors. *Nat. Commun.* **10**, 2615–2618 (2019).
49. Wang, Y. et al. In-situ generation of large numbers of genetic combinations for metabolic reprogramming via CRISPR-guided base editing. *Nat. Commun.* **12**, 678 (2021).
50. Lian, J., HamediRad, M., Hu, S. & Zhao, H. Combinatorial metabolic engineering using an orthogonal tri-functional CRISPR system. *Nat. Commun.* **8**, 1688 (2017).
51. Binder, S. et al. A high-throughput approach to identify genomic variants of bacterial metabolite producers at the single-cell level. *Genome Biol.* **13**, R40 (2012).

52. Teng, Y. et al. Biosensor-enabled pathway optimization in metabolic engineering. *Curr. Opin. Biotechnol.* **75**, 102696 (2022).
53. Zhou, L. et al. Unlocking the potential of enzyme engineering via rational computational design strategies. *Biotechnol. Adv.* **73**, 108376 (2024).
54. Ye, M. et al. Promoter engineering enables precise metabolic regulation towards efficient beta-elemene production in *Ogataea polymorpha*. *Synth. Syst. Biotechnol.* **9**, 234–241 (2024).
55. Hossain, A. et al. Automated design of thousands of nonrepetitive parts for engineering stable genetic systems. *Nat. Biotechnol.* **38**, 1466–1475 (2020).
56. Shimazaki, S., Yamada, R., Yamamoto, Y., Matsumoto, T. & Ogino, H. Building a machine-learning model to predict optimal mevalonate pathway gene expression levels for efficient production of a carotenoid in yeast. *Biotechnol. J.* **19**, e2300285 (2024).
57. Huang, Z. R. et al. Enhanced single-base mutation diversity by the combination of cytidine deaminase with DNA-repairing enzymes in yeast. *Biotechnol. J.* **18**, e2300137 (2023).
58. Choi, K. R. et al. Systems metabolic engineering strategies: integrating systems and synthetic biology with metabolic engineering. *Trends Biotechnol.* **37**, 817–837 (2019).
59. Zhou, S., Ding, N., Han, R. & Deng, Y. Metabolic engineering and fermentation optimization strategies for producing organic acids of the tricarboxylic acid cycle by microbial cell factories. *Bioresour. Technol.* **379**, 128986 (2023).
60. Weinberg, B. H. et al. Large-scale design of robust genetic circuits with multiple inputs and outputs for mammalian cells. *Nat. Biotechnol.* **35**, 453–462 (2017).
61. Friedland, A. E. et al. Synthetic gene networks that count. *Science* **324**, 1199–1202 (2009).
62. Ma, H., Kunes, S., Schatz, P. J. & Botstein, D. Plasmid construction by homologous recombination in yeast. *Gene* **58**, 201–216 (1987).
63. Gietz, R. D. & Woods, R. A. Transformation of yeast by lithium acetate/single-stranded carrier DNA/polyethylene glycol method. *Methods Enzymol.* **350**, 87–96 (2002).
64. Holm, C., Meeks-Wagner, D. W., Fangman, W. L. & Botstein, D. A rapid, efficient method for isolating DNA from yeast. *Gene* **42**, 169–173 (1986).
65. Yuan, S., Chan, H. C. S. & Hu, Z. Using PyMOL as a platform for computational drug design. *Wiley Interdiscip. Rev. Comput. Mol. Sci.* **7**, e1298 (2017).

Acknowledgements

This work was supported by funding from the National Key R&D Program of China, Synthetic Biology Research [2019YFA0903800 for Y.W. and G.R.Z], the National Natural Science Foundation of China [32471483 for Y.W.], the Natural Science Foundation of Tianjin [23JCYBJC00220 for Y.W.].

Author contributions

Y.W., Y.-J.Y., Y.M., and G.-R.Z. conceptualized the study. Y.W., J.Y.L., S.M.G., and Y.M. designed the experiments. J.Y.L., S.M.G., P.Y.H., Z.H.F., X.Y.H., N.W., H.Z.T., and T.Y.Y. formed the experiments. S.M.G., J.Y.L., and X.Y.Z. analyzed the data. S.M.G, J.Y.L., and Y.W. wrote the manuscript. Y.-J.Y. supervised all aspects of the study.

Competing interests

The authors declare no competing interests.

Additional information

Supplementary information The online version contains supplementary material available at https://doi.org/10.1038/s41467-025-57206-w.

Correspondence and requests for materials should be addressed to Yi Wu.

Peer review information *Nature Communications* thanks Gita Naseri, Zi-Xu Zhang and the other, anonymous, reviewer(s) for their contribution to the peer review of this work. A peer review file is available.